Probing the electronic structure of complex crystals with electron energy loss spectroscopy: a study of *natisites*

2006 J. Phys.: Condens. Matter 18 3629

(http://iopscience.iop.org/0953-8984/18/15/009)

INSTITUTE OF PHYSICS PUBLISHING JOURNAL OF PHYSICS: CONDENSED MATTER

J. Phys.: Condens. Matter **18** (2006) 3629–3637 doi:10.1088/0953-8984/18/15/009

Probing the electronic structure of complex crystals with electron energy loss spectroscopy: a study of *natisites*

G Radtke and G A Botton

Brockhouse Institute for Materials Research, McMaster University, 1280 Main Street West, Hamilton, L8S 4M1, ON, Canada

E-mail: gbotton@mcmaster.ca

Received 16 January 2006
Published 30 March 2006
Online at stacks.iop.org/JPhysCM/18/3629

Abstract

The energy loss near edge structure (ELNES) of the O K and Ti L_{23} edges recorded in two compounds with the *natisite* structure, namely $Li_2TiOSiO_4$ and $Li_2TiOGeO_4$, are interpreted using *ab initio* band structure and ligand-field multiplet calculations. The origin of the different peaks observed in the experimental O K edge is discussed in terms of chemical bonding between the O atoms and their Ti and Si (Ge) nearest neighbours. In particular, the high sensitivity of the O K edge to the square pyramidal geometry of the Ti atomic site is underlined and correlated to the signature observed on the Ti L_{23} edge. We demonstrate here the ability of electron energy loss spectroscopy to investigate the chemical and structural environment of atoms in complex compounds.

1. Introduction

Electron energy loss spectroscopy (EELS) in the transmission electron microscope (TEM) is one of the most powerful solid-state spectroscopies dedicated to the study of the electronic structure of materials. With the increasing emphasis on spatially resolved measurements on defects or interfaces, it becomes crucial to fully understand all spectral features in terms of the local geometry and bonding around the excited atom. In this framework, it is particularly interesting to investigate the experimental signature of atoms in complex environments and try to understand the influence of the different parameters such as the symmetry of the atomic site or the nature of the neighbouring atoms on the spectral shape. In this paper, we present the theoretical analysis of the O K and Ti L_{23} edges recorded in bulk $Li_2TiOSiO_4$ and $Li_2TiOGeO_4$. The experimental spectra have already been published in a previous paper [1] and interpreted qualitatively by comparison to O K edges recorded in reference compounds. However, this simple approach introduced inaccuracies in the discussion of the experimental results. The goal

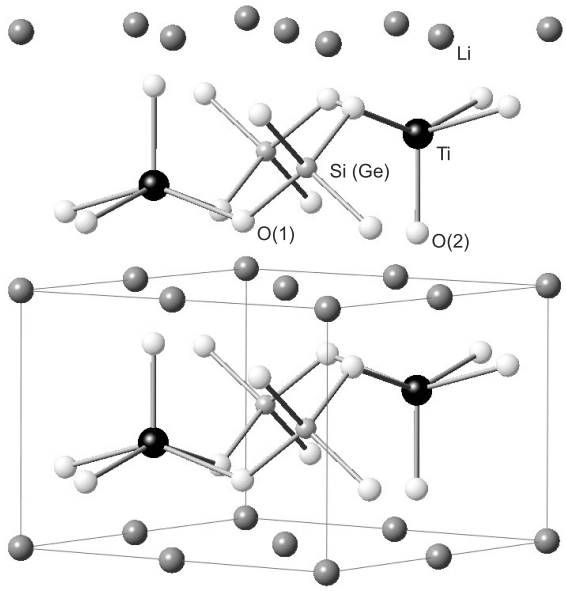

Figure 1. The crystallographic structure of *natisite*: the layers of corner sharing SiO_4 (GeO_4) tetrahedra and TiO_5 square pyramids are separated by planes of Li.

of this paper is firstly to clarify the origin of the different peaks observed in the experimental spectra using *ab initio* band structure calculations and, in particular, to discuss the crucial influence of the crystal structure on the spectral shape. The second interesting point of this work is thus to correlate the signatures observed on both O K and Ti L_{23} edges with the peculiar fivefold coordination of Ti. These compounds are indeed of particular interest mainly because 80% of their O atoms are shared between SiO_4 (GeO_4) tetrahedra and TiO_5 square pyramidal groups. Their first coordination shell is therefore constituted by a Ti and by a Si (Ge) atom [2, 3].

$Li_2TiOSiO_4$ and $Li_2TiOGeO_4$, like other compounds of general formula A_2MXO_5 with A a monovalent cation and M a tetravalent cation (see for example [1–5]), adopt the *natisite* structure. This structure (figure 1) can be simply described as a superposition of layers of corner-sharing SiO_4 (GeO_4) tetrahedra and TiO_5 square pyramids, the $TiSiO_5^{2-}$ ($TiGeO_5^{2-}$) sheets being bound by planes of Li^+ cations. The Si (Ge) atoms are in the centre of O(1) tetrahedra with equal bond lengths of 1.63 Å. These O(1) atoms are shared with the Ti square pyramids and form their basal plane. The distance between the central Ti and the four O(1) atoms is equal to 1.97 Å. A second inequivalent O(2) atom located at the apex of the Ti completes the pyramid with a substantially shorter Ti–O(2) distance of 1.70 Å. The O(2) of the adjacent layer can also be used to form a distorted octahedron around the Ti atoms, the distance separating these last two atoms being 2.70 Å.

Electron energy loss spectroscopy is a well adapted tool to investigate the complex electronic structure of these compounds. The O K edge in particular arises from transitions from the 1s core state to unoccupied states of p symmetry located on the O sites [6]. It is thus very sensitive to the *local electronic structure* and especially to the chemical bond formed between O atoms and their neighbours. The Ti L_{23} edge is dominated by atomic multiplet effects [7] with, however, a strong sensitivity to the symmetry of the surrounding crystal field. This edge is therefore a powerful probe of the formal valency and the coordination of the transition metal atoms.

2. Materials and methods

The experimental spectra were acquired on a dedicated UHV scanning transmission electron microscope (VG HB501) equipped with a Gatan energy-loss spectrometer (GIF model UHV 678) allowing an energy resolution of 0.4–0.5 eV. The TEM samples were prepared by crushing the powders in ethanol and by dispersing the suspension on a holey carbon-covered Cu grid. All the details about the sample preparation can be found in section 2 of a previous paper [1].

Electronic structure calculations have been carried out using the Wien2k code [8]. This code uses the augmented plane wave + local orbital method (APW+lo) in the framework of the density-functional theory [9, 10]. The generalized gradient approximation (GGA) [11] has been used for the exchange–correlation potential and muffin-tin radii were chosen as $R_{\mathrm{mt}}(\mathrm{O}) = 1.5$ au, $R_{\mathrm{mt}}(\mathrm{Ti}) = 1.7$ au, $R_{\mathrm{mt}}(\mathrm{Li}) = 1.9$ au, and $R_{\mathrm{mt}}(\mathrm{Si, Ge}) = 1.5$ au, the plane wave cut-off parameter RK_{max} as 7.0 and l_{max} as 10. The number of k-points used in the first Brillouin zone was increased until convergence of the total DOS was achieved. We focused this work on the study of the unoccupied states up to 25 eV above the Fermi level. After the self-consistent calculation of the electron density, the basis set was improved to calculate these unoccupied states more accurately by increasing the energy of the APWs. Experimental lattice parameters and reduced atomic coordinates obtained from x-ray diffraction [2, 3] were used in these calculations. The O K edges have been calculated in the dipole approximation using the TELNES module according to the formalism described in [12]. The energy spread of the electron source was included through a Gaussian broadening of 0.5 eV full width at half maximum (FWHM). Excitation finite lifetime broadenings were taken into account in the following way: a constant Lorentzian broadening of FWHM 0.14 eV [13] was used to model the core–hole finite lifetime and an energy-dependent Lorentzian broadening using the empirical relation proposed in [14] to model the quasi-particle finite lifetime. The theoretical work of Hébert *et al* [15] confirmed the correctness of this approximation at least in the first 15 eV after the edge onset, i.e. the energy region concerned by this work.

Finally, the Ti L_{23} edge has been calculated in the framework of the ligand-field multiplet theory [7]. This edge corresponds to the excitation of a 2p core electron mainly to the unoccupied 3d states, i.e. to the transition from a $2p^6 3d^0$ ground state to a $2p^5 3d^1$ excited electronic configuration of the Ti^{4+} ion. In addition to the Gaussian broadening used to account for the experimental resolution, individual Lorentzian broadenings have been applied for each of the four main lines constituting the spectrum according to the procedure described in [16].

3. Results

3.1. The O K edge

The O K edge recorded in $Li_2TiOSiO_4$ is displayed in figure 2. The experimental spectrum is constituted by four prominent peaks labelled (A)–(A′), (B), (C) and (D) in the figure. On a finer scale, the first peak shows an asymmetric shape arising from two contributions of similar intensities and separated by 1 eV at 528 and 529 eV and indicated by the labels (A) and (A′) on the figure. Three other peaks appear clearly at 531, 535.5 and 539 eV respectively. A last broad feature labelled (E) is still visible at 546 eV. The theoretical spectrum is shown in the same figure. This spectrum has been calculated by summing the individual contributions corresponding to the inequivalent O(1) and O(2) atoms with a relative weight of 0.8 and 0.2 respectively. These individual components are shown on the top left inset of the same figure. As can be seen, the spectral shape is dominated by the O(1) contribution and the only significant modification due to the O(2) is the reinforcement of peak (A′). Using this procedure, the overall

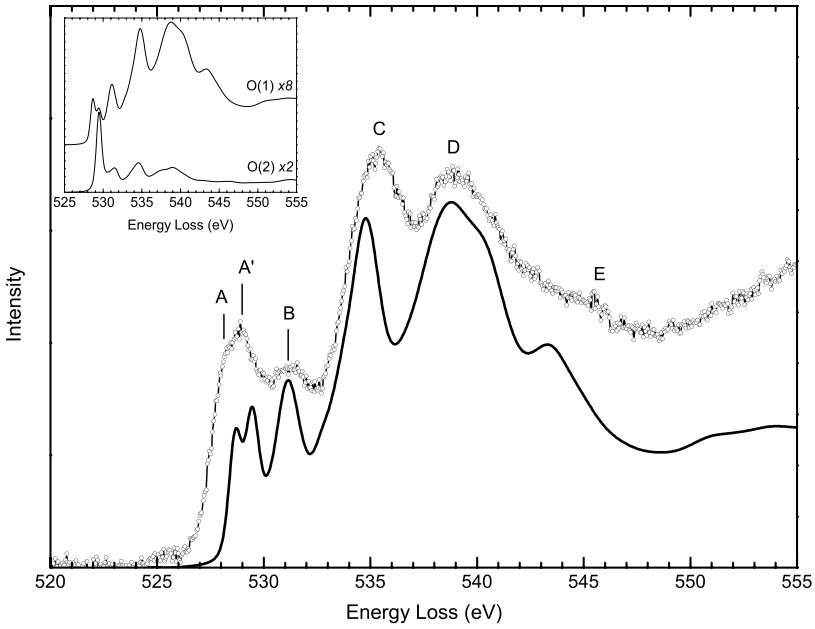

Figure 2. Comparison between experimental (dots) and theoretical (full line) O K edges in $Li_2TiOSiO_4$. The individual contributions calculated for O(1) and O(2) are shown in the top left inset.

agreement obtained between theoretical and experimental spectra is very good. In particular, the double structure (A) and (A′) is clearly reproduced. The main discrepancies come from an approximate prediction of the relative energy position and intensities for some of the peaks.

The same analysis has been applied to the O K edge in $Li_2TiOGeO_4$ (figure 3). Even if the shape of the experimental spectrum is relatively different from $Li_2TiOGeO_4$, it is important to notice that its basic structure remains the same. To emphasize this point, we used the same labels in figures 2 and 3. The double peak (A)–(A′) is still present at the edge onset, but in this compound (A′) only appears as a shoulder of the following peak (B) at 533 eV. The intensity of peak (B) is greatly increased with respect to $Li_2TiOSiO_4$. Finally, the same intense features, labelled (C) and (D), are found at 535 and 541 eV before the broad structure (E) at 545 eV. Therefore, besides the small variations in intensity and energy positions of the peaks, these two spectra exhibit the same global structure as can be expected from the similarity in their structure and chemistry. Again, the theoretical spectrum shows a fairly good agreement with the experimental data even if the energy position and the shape of certain peaks are not exactly reproduced. In particular, the trends observed in the experiments are confirmed by the calculations: the intensity of peak (B) is increased with respect to the other peaks and the energy separation between peaks (C) and (D) is more important than in $Li_2TiOSiO_4$. The double structure (A) and (A′) is still clearly visible, the intensity of peak (A′) being again enhanced by the O(2) contribution.

Different parameters may explain the remaining discrepancies observed between experimental and theoretical spectra [6]. One of the most important here is that the core hole created by the loss event was not taken into account in our calculations. The main effect of the missing electron on the tightly bound core state is to create a local, more attractive potential. This modification of the potential leads generally to a modification of the probed unoccupied electronic states and therefore to a modification of the fine structure. A second reason arises

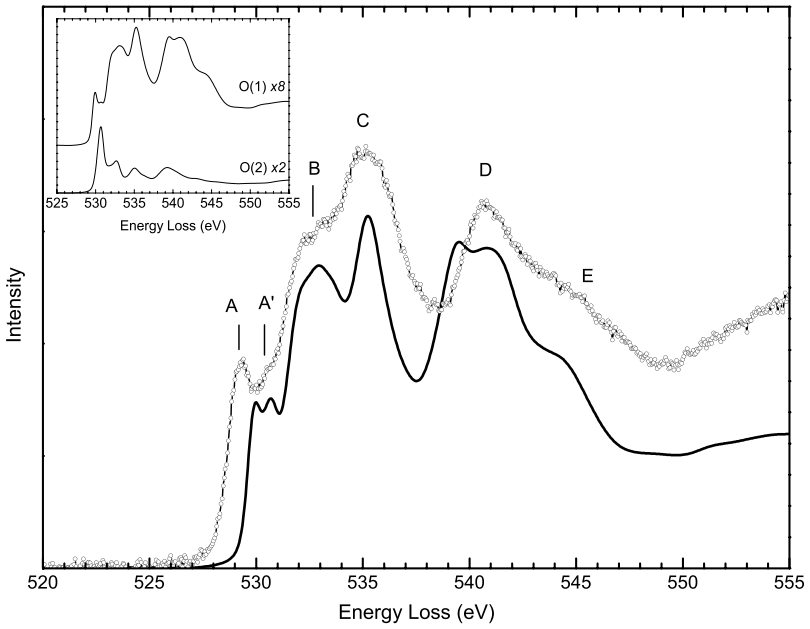

Figure 3. Comparison between experimental and theoretical O K edge in $Li_2TiOGeO_4$. The individual contributions calculated for O(1) and O(2) are shown in the top left inset.

from the impossibility of calculating accurate threshold energies [17] and then determining precisely the relative positions of the individual contributions corresponding to O(1) and O(2). In this work, these two contributions have been summed directly from the same ground-state energy scale but variations due especially to the difference in the local environments of these atoms and thus to a difference of the core-hole screening can be expected. In the present case, however, the overall agreement with the experimental spectra allows further unambiguous analysis and interpretation of the O K edge fine structure.

3.2. Electronic structure calculation

The total and projected densities of states calculated for $Li_2TiOSiO_4$ and $Li_2TiOGeO_4$ are presented in figures 4(a) and (b) respectively. These compounds are insulators with bandgaps of 3.3 and 3.5 eV respectively separating a valence band of 7 eV width of dominant O 2p character from the conduction band. We will focus our discussion on the structure of this conduction band as we are primarily interested by the unoccupied states. The bottom of this band is dominated by the Ti 3d states. These states extend over 4 eV and can be divided into three distinct contributions: two sharp and intense peaks at 3–4 eV and 4–5 eV above the Fermi level followed by a broader band between 5 and 7 eV. In order to understand the origin of these structures, we can start with the electronic structure of an elementary polyhedron constituted by a Ti atom surrounded by its first coordination shell of oxygen and use a simple approach based on crystal-field theory. The initially fivefold degenerate 3d states of the Ti atom are split into two distinct subsets under the influence of a perfect octahedron (of O_h symmetry) constituted by six oxygen atoms carrying a negative charge as summarized in figure 5. These two sets transform according to the e_g and t_{2g} irreducible representations of the cubic point group and are respectively spanned by the $(d_{z^2}, d_{x^2-y^2})$ and (d_{xy}, d_{yz}, d_{xz}) orbitals. The

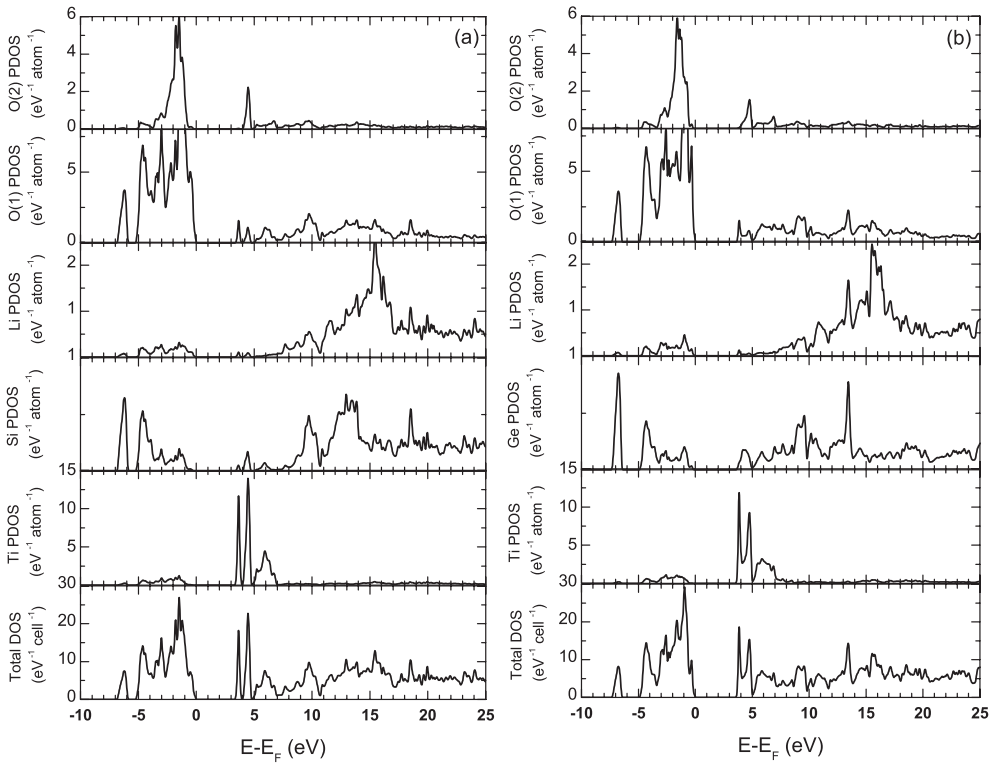

Figure 4. Total and projected densities of states (DOS) calculated in (a) $Li_2TiOSiO_4$ and (b) $Li_2TiOGeO_4$.

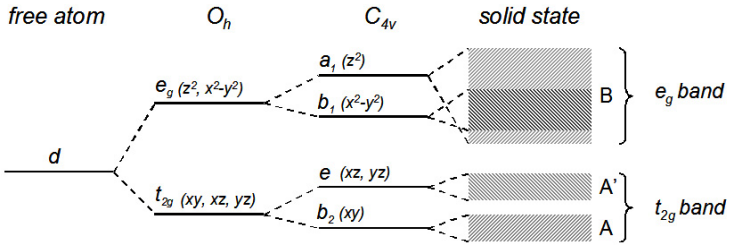

Figure 5. Schematic energy levels of Ti 3d states in O_h crystal field, tetragonal C_{4v} symmetry and in bulk *natisites*. This diagram explains qualitatively the origin of peaks (A), (A′) and (B) observed at the O K edge of $Li_2TiOSiO_4$ and $Li_2TiOGeO_4$.

e_g states are higher in energy due to the fact that the orbitals are pointing towards the ligand atoms, thus experiencing a strong electrostatic repulsion. The t_{2g} orbitals point between the oxygen atoms and have therefore a lower energy. In *natisites*, the octahedron of oxygen atoms around the Ti is distorted in such a way that only five atoms are still present in the first coordination shell, forming a square pyramid around the transition metal atom. The symmetry of the Ti atom site is now lowered to the tetragonal C_{4v} point group (a sub-group of D_{4h}), leading to a further splitting of the e_g states into two one-dimensional subsets, of a_1 and b_1 symmetries respectively spanned by (d_{z^2}) and ($d_{x^2-y^2}$) orbitals and of the t_{2g} states in a one-dimensional set b_2 spanned by the (d_{xy}) orbital and in a two-dimensional set *e* spanned by the

remaining (d_{xz}, d_{yz}) orbitals. The geometry of the pyramid corresponds to a compression of the Ti–O(2) bond length (1.70 Å) along the z direction by comparison to the Ti–O(1) distance of 1.97 Å. In terms of electrostatic repulsion, we can expect the b_2 states to be lower in energy with respect to the e states as well as the b_1 to be lower in energy with respect to the a_1 states, as a result of this specific distortion. This is simply justified by the relative stabilization of the orbitals lying in the (x, y) plane as the Ti–O(1) interatomic distance is longer than the Ti–O(2) distance by 15%. This crystal field approach is obviously not complete. The hybridization between Ti 3d and O 2p and the energy dispersion due to the band formation in the solid state has to be included in our description. In this case, the small overlap characteristic of the π interaction leads to a small dispersion (of about 1 eV) for the (d_{xy}) and (d_{xz}, d_{yz}) band, thus forming the two distinct sharp peaks at the bottom of the conduction band. The stronger σ interaction in the case of (d_{z^2}) and ($d_{x^2-y^2}$) bands leads to the formation of the 2 eV width band at higher energy. However, the displacement of the Ti atom out of the O_4 basal plane leads to a substantial reduction of the hybridization in the case of the ($d_{x^2-y^2}$) band. This overall structure is reflected in the O 2p projected density of states (PDOS) for O(1) and to a lesser extent for O(2). This analysis allows us to attribute a precise origin to the first peaks of the O K edge. The (A)–(A′) structure is essentially due to the hybridization of O 2p with Ti 3d states of t_{2g} symmetry. The double structure visible on the experimental edge and reproduced in the simulated spectrum arises directly from the lower symmetry of the square pyramidal environment of the Ti atoms with respect to a perfect octahedron, leading to a further splitting of the t_{2g} states. The second peak, labelled (B) in figures 2 and 3, can be attributed to the strong interaction of O 2p with Ti 3d states of e_g symmetry. These strong features observed at the bottom of the conduction band are followed at higher energy by the Si or Ge states. Two peaks are clearly visible in the Si PDOS at 9–10 eV and 12–14 eV above the Fermi level with a Si 3sp character and in the Ge PDOS at 9 eV and 13–14 eV with a Ge 4sp character. These peaks are also visible in the O PDOS and are thus related to the strong Si–O (Ge–O) covalent bonding responsible for the presence of SiO_4 (GeO_4) tetrahedra in these compounds. As a consequence, peaks (C) and (D) corresponding to these energies can be mainly attributed to the hybridization between O 2p and Si 3sp (Ge 4sp) states. This attribution is however not as clear as in the case of peaks (A), (A′) and (B). Indeed, the interaction between O 2p and Ti 4sp or Li p states arising in the same energy range cannot be neglected and participate in the formation of peak (D). A last comment should be made concerning the very different contribution of O(2). This atom is located at the top of the pyramid and interacts mainly with the central Ti atom. The O(2) PDOS thus exhibits strong features at the bottom of the conduction band. In particular, the strong π interaction between the Ti d_{xz} and d_{yz} and the O(2) p_x and p_y orbitals leads to the prominent peak (A′) between 529 and 530 eV visible in the individual components shown in figures 2 and 3.

3.3. The Ti L_{23} edge

The Ti L_{23} edges recorded in the same compounds are shown in figure 6. The spectral shape is dominated by the Ti 2p core–hole spin–orbit coupling that splits the edge into two main parts separated by about 5 eV, namely the L_3 and L_2 edges, as indicated in the figure. Each of these lines is further split into two peaks separated by about 2 eV and mainly due to the effect of the crystal field on the Ti 3d orbitals. These structures cannot be understood in terms of the one-electron model used to describe the O K edge and a quantitative description can only be achieved using an approach based on ligand-field multiplet theory. The spectrum calculated for a Ti^{4+} ion in crystal field of D_{4h} symmetry in shown in the same figure. This approximation of the crystal field symmetry is justified by the fact that the dominant factor is the tetragonal distortion, the lower symmetry of the crystal (C_{4v}) having a negligible influence on

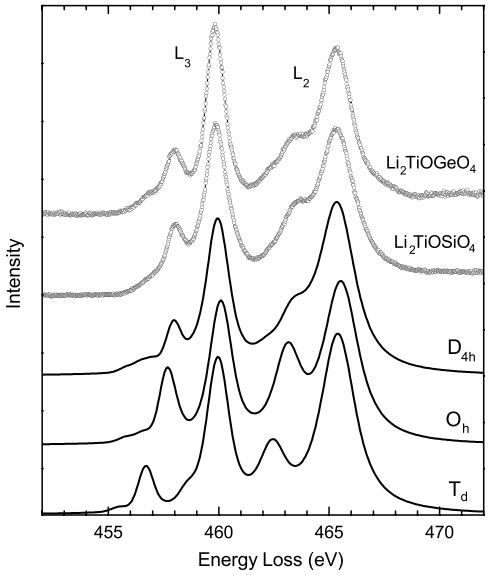

Figure 6. Comparison between experimental Ti L_{23} edges recorded in $Li_2TiOSiO_4$ and $Li_2TiOGeO_4$ and ligand-field multiplet calculations for Ti^{4+} in different symmetries. The experimental spectra for both compounds are only consistent with a tetragonal distortion.

the spectral shape. The fitting parameters of the multiplet model are here the three parameters D_q, D_s and D_t [18] needed to describe the crystal field surrounding the transition metal atom. In this study, they have been determined with the help of the results of the *ab initio* calculations shown in the previous section. In particular, care has been taken to reproduce the one-electron orbital energy level ordering shown in figure 5 with a t_{2g}–e_g splitting of 2 eV and an e–b_2 subsplitting of the t_{2g} level of 1 eV. Values of 0.2 eV for D_q, −0.21 eV for D_s and 0.07 eV for D_t are consistent with these constraints and lead to the excellent agreement shown in figure 6. It is well known that the symmetry of the crystal field has a very strong influence on the line shape of tetravalent titanium [19]. In order to illustrate its effect, spectra calculated with the same value for the crystal field parameter D_q (0.2 eV) in both octahedral and tetrahedral symmetries are also displayed in the figure. This simple comparison leads to an unambiguous confirmation of the tetragonal symmetry of the Ti atomic site in *natisites*. Finally, Ti in fivefold coordination also occurs in mineral *fresnoite* $Ba_2TiOSi_2O_7$, where the reported Ti L_{23} edge studied in x-ray absorption spectroscopy shows a very similar shape [20].

The excellent agreement observed between the experimental Ti L_{23} edges recorded in *natisites* and both the theoretical ligand-field multiplet calculation of Ti^{4+} in tetragonal symmetry and the experimental spectrum recorded in a compound with fivefold coordinated Ti confirms the presence of a square pyramidal Ti atomic site in these compounds. The most interesting point here is that the values of the crystal field parameters required to reproduce the experimental spectrum are consistent with the one-electron orbital energy levels ordering found in our *ab initio* calculations. The O K and the Ti L_{23} edges are thus two consistent probes reflecting the same peculiar symmetry of the Ti atomic site.

4. Conclusion

In this paper, *ab initio* band structure and ligand-field multiplet calculations have been used to interpret the fine structure of the O K and the Ti L_{23} edges recorded in two compounds

adopting the *natisite* structure, $Li_2TiOSiO_4$ and $Li_2TiOGeO_4$. The first part of the O K edge is constituted by three peaks related to the hybridization between Ti 3d and O 2p states. More specifically, the peculiar symmetry of the Ti site, a square pyramid of the C_{4v} point group, is responsible for a further splitting of the t_{2g} states leading to the observation of two peaks (A) and (A′) in the experimental spectra. The structures (C) and (D) at higher energies are essentially due to the hybridization between O 2p and Si (Ge) sp states. The fine structure observed at the Ti L_{23} edge has been successfully interpreted using a ligand-field multiplet accounting for the tetragonal symmetry of the atomic site and confirms nicely the interpretation of the O K edge. Through this work, we have demonstrated that the use of adapted theoretical models to interpret the O K and Ti L_{23} edge fine structures, combining band structure and ligand-field multiplet, gives a strong insight into the atomic and electronic structure of these materials. The ionization edges recorded in EELS thus appear as potential powerful probes of the local atomic and electronic structure in complex materials, especially in the field of interfaces due to changes in coordination and the presence of bridging atoms between structures.

Acknowledgment

We thank the Natural Science and Engineering Research Council (Canada) for funding and Profs H Withfield, T Bastow and J Etheridge for stimulating the initial work on these compounds.

References

[1] Bastow T J, Botton G A, Etheridge J, Smith M E and Withfield H J 1999 *Acta Crystallogr.* A **55** 127
[2] Ziadi A, Thiele G and Elouadi B 1994 *J. Solid State Chem.* **109** 112
[3] Kireev V V, Yakubovich O V, Ivanov-Shits A K, Mel'nikov O K, Dem'yanets L N, Skunman J and Chaban N G 2001 *Russ. J. Coord. Chem.* **27** 34
[4] Nyman H and O'Keeffe M 1978 *Acta Crystallogr.* B **34** 905
[5] Rangan K K, Piffard Y, Joubert O and Tournoux M 1998 *Acta Crystallogr.* C **54** 176
[6] Paxton A T 2005 *J. Electron. Spectrosc. Relat. Phenom.* **143** 51
[7] De Groot F 2005 *Coord. Chem. Rev.* **249** 31
[8] Blaha P, Schwarz K, Madsen G, Kvasnicka D and Luitz J 2001 *Wien2k, An Augmented Plane Wave Plus Local Orbitals Program for Calculating Crystal Properties* Vienna University of Technology, Inst. of Physical and Theoretical Chemistry
[9] Hohenberg P C and Kohn W 1964 *Phys. Rev.* **136** B864
[10] Kohn W and Sham L J 1965 *Phys. Rev.* **140** A1133
[11] Perdew J P, Burke K and Ernzerhof M 1996 *Phys. Rev. Lett.* **77** 3865
[12] Hébert-Souche C, Louf P-H, Blaha P, Nelhiebel M, Luitz J, Schattschneider P, Schwarz K and Jouffrey B 2000 *Ultramicroscopy* **83** 9
[13] Domke M 1990 *Chem. Phys. Lett.* **173** 122
[14] Weijs P J, Czyżyk M T, van Acker J F, Speier W, Goedkoop J B, van Leuken H, Hendrix H J M, de Groot R A, van der Laan G, Buschow K H J, Wiech G and Fuggle J C 1990 *Phys. Rev.* B **41** 11899
[15] Hébert C, Kostner M and Schattschneider P 2000 *Conf. Proc. EUREM XII (Brno)* p 333
[16] De Groot F M F, Fuggle J C, Thole B T and Sawatzky G A 1990 *Phys. Rev.* B **41** 928
[17] Paxton A T, van Schilfgaarde M, MacKenzie M and Craven A J 2000 *J. Phys.: Condens. Matter* **12** 729
[18] Ballhausen C J 1962 *Introduction to Ligand Field Theory* (New York: McGraw-Hill) p 99
[19] De Groot F M F, Figueiredo M O, Basto M J, Abbate M, Petersen H and Fuggle J C 1992 *Phys. Chem. Minerals* **19** 140
[20] Schofield P F, Henderson C M B, Cressey G and van der Laan G 1995 *J. Synchrotron Radiat.* **2** 93